ON FUNCTIONAL NETWORK CONNECTIVITY IN FOCAL NEOCORTICAL SEIZURES USING BELIEF-PROPAGATION METRICS

Thomais Asvestopoulou [⋆†] *Maria Markaki* [⋆] *Joseph Lombardo* [‡]
Stelios Manolis Smirnakis [‡] Maria Papadopouli [⋆†]

[⋆] Institute of Computer Science, Foundation for Research and Technology-Hellas, Heraklion, Greece
[†] Department of Computer Science, University of Crete, Heraklion, Greece
[‡] Department of Neurology, BW's & JP VA Hospitals, Harvard Medical School, Boston, USA

ABSTRACT

Epilepsy affects 2-3% of the population. To study the emergence and spread of focally initiated seizures, we used the 4-aminopyridine (4-AP) model, a well-established, reliable, model of acute focal neocortical seizures. We examined the activity profiles of individual neurons in layer 2/3 (L2/3) of the visual cortex during focal seizures induced following intracortical 4-AP injections. Here we characterize the functional network connectivity using graph-theoretical metrics, such as normalized degree of connectivity, clustering coefficient, and weighted clustering coefficient. To capture the contribution and influence of a neuron to the connectivity of the network within a larger region, we introduce the *affinity*, a belief-propagation-based metric, that integrates the pairwise temporal correlation of the firing events of neurons in a subnetwork. Our analysis reveals the structure of the functional networks after the 4-AP injection, the significant increase of the temporal correlation of neurons, highlighting the influence of neurons in the region close to the 4-AP injection. It comparatively analyzes the findings with other network architectures, including the functional network of the control (i.e., healthy mouse, prior to the injection) as well as graphs with well-defined structure.

Index Terms— focal neocortical seizures, network analysis, STTC, temporal correlation, belief propagation

1. INTRODUCTION

Epilepsy affects 2-3% of the population. Brain-injury patients carry high-risk of epilepsy for decades following injury [1], causing morbidity. Injury causing epilepsy typically leads to excitation/inhibition imbalance, which drives neural-circuits into self-perpetuating oscillatory activity-states, feeding the hyper-synchronous epileptic-bursts seen on cortical-surface EEG [2, 3]. Our understanding of how neurons interact to generate the abnormal network activity patterns that underlie ictogenesis is limited [4]. Seizures involve the generation and propagation of hyper-synchronous activity across cortical-circuits. It is important to understand what changes in the cortical circuit allow a highly-correlated firing state to emerge, evolve, and recur after focal-cortical injury. How do mechanisms that regulate neuronal network activity in-vivo fail? Interneurons are important in regulating the activity of pyramidal neurons. In normal mice, we found that spontaneous activity patterns obey certain organization rules, e.g. specific groups of pyramidal neurons get activated-together and inhibited-together by specific neighboring interneurons [5]. Neurons within each layer do not fire independently from each other but rather form computationally meaningful interconnected neuronal ensembles [6, 7].

Temporal correlations in neuronal spike trains are key in characterizing the functional connectivity. We extended the spike time tiling coefficient (STTC) [8], a metric superior to commonly used measures, as it accounts for relative time shifts, local fluctuations, and presence of periods without firing events, to incorporate the order in temporal correlation of the firing events between neurons. Two neurons are functionally connected (i.e., by an edge in the corresponding graph), if their firing activity has a statistically significant STTC value (temporal correlation). The identification of patterns of functional connectivity reflects underlying direct or indirect interaction across pairs of neurons.

To characterize the functional connectivity in the context of the 4-aminopyridine (4-AP) model, a well-established, reliable, model of acute focal neocortical seizures, we design and apply new network metrics appropriate for our objectives: metrics that can be used in weighted directed networks to reveal its structure, capture the influence of neurons on other neurons and spatial locality of the propagation of the information, and adequately treat the heterogeneity in strengths and asymmetries between neurons. We identify the structure and the robust components of a network, i.e., subnetworks that remain the same, and quantify the amount and significance of changes as a specific network evolves in time (e.g., before vs. post 4-AP injection), using graph-theoretical metrics, such as the normalized degree of connectivity (DoC), clustering coefficient (CC), and weighted clustering coefficient (WCC). The clustering coefficient of a node, defined as the

fraction of a node's pairs of neighbours that are connected, indicates how tightly connected its neighboring nodes are. The weighted clustering coefficient has been estimated on the corresponding weighted graph, where the weight of an edge is the STTC value of the corresponding neurons (connected by that edge). In addition to the aforementioned metrics, which are "local", we introduce the *affinity*, a belief-propagation (BP) based metric, to capture the contribution or influence of a neuron considering a *wider area around that neuron*, its sub-network (e.g., within a range of 10-hop away neighbor neurons). The BP, an efficient inference algorithm on probabilistic graphical models, has been successfully applied to numerous domains, including error-correcting codes, stereo imaging in computer vision, fraud detection, and malware detection ([9] and references therein). It uses the principle of "homophily", i.e., the general assumption that neighbors influence each other.Here, homophily indicates the membership to the same neural ensemble. To the best of our knowledge, this is the first time that a BP metric is used to reveal the neuronal ensembles and functional connectivity structure, in general, as well as, specifically, in the context of focal neocortical seizures. Indirectly, here the affinity enables us to cluster the neurons in an unsupervised manner, by identifying their membership in a class/subnetwork (e.g., participation in seizure subnetworks in this context). To highlight specific features of the functional connectivity in 4-AP, we also compare it with different network architectures (e.g., control, null, Erdös-Rényi random network, lattice).

This work analyzes datasets obtained from one mouse, during spontaneous conditions, before the 4-AP injection and post 4-AP injection. It shows the high temporal correlation of neurons in the context of post 4-AP and its denser functional network connectivity, compared to other network architectures and conditions. Moreover, it demonstrates the power of the weighted affinity to identify neurons that seem to play an important role in the evolution of the ictogenesis. Section 2 briefly overviews the prior work, while Section 3 presents the data acquisition and preprocessing. In Section 2, we briefly overview the related work. Section 4 presents our main methods and highlights the main results. In, Section 5, we summarize our main conclusions and future work plans.

2. RELATED WORK

Cortical injections of chemoconvulsants are thought to induce a focus of epileptiform activity from where seizures propagate in the surrounding network [10]. Epileptiform activity in this surrounding network (often referred to as propagation area) have been shown to engage cortical neurons in a spatio-temporal ordered fashion [11], suggesting that neurons that are physically closer to the injection site get recruited earlier than neurons located at a larger physical distance. In a follow-up study [12], the recruitment of neurons at the level of the injection site was compared with the recruitment of neurons in the propagation area. In such study, the recruitment of large proportion of neurons in the initiation site appeared to occur simultaneously (at the temporal resolution of the recordings), suggesting that the engagement of neurons in the injection site might not only be determined by their physical distance. Using wide-field calcium imaging, Rossi *et al.* [13] have shown that also brain areas at a larger distance to the initiation site might get recruited earlier than areas physically closer to it depending on their homotopic connections to the injection site areas. Whether similar rules govern recruitment in the injection area as well is to be determined.

To the best of our knowledge, this is the first study that discusses the functional network connectivity in the context of 4-AP. In our prior work [14], we have examined the functional network connectivity in absence seizures. Absence epilepsy interrupts normal cortical processing, producing reversible episodes of altered consciousness. During interictal activity, most neurons are functionally connected with a large number of neighbors within the FoV, while in seizure epochs, the connectivity is reduced substantially. The evolution of ictogenesis in 4-AP differs substantially from the absence epilepsy. Here, this methodology has been extended using the weighted clustering coefficient [15] and belief propagation algorithms [9].

3. DATA ACQUISITION AND PREPROCESSING

Experiment was performed on an adult (>8 weeks old) Thy1-GaMP6s (C57BL/6J-Tg (Thy1-GCaMP6s) GP4.3Dkim/J) mouse which expresses the GCaMP6s calcium indicator in pyramidal neurons [16]. Two-photon calcium imaging was performed using an in vivo Ultima multiphoton microscope (Bruker, Madison, WI) equipped with a Ti:Sapphire Insight pulsed laser (Sprectra Physics, Santa Clara, CA). Calciumm signals were imaged through a 16x water immersion lens (Nikon, Tokyo, Japan; 0.8 NA, 3 mm working distance) by exciting the genetically encoded GCaMP6s at 920 nm. The field of view (FoV) was scanned in spiral mode at approximately 5 Hz. We imaged layer 2/3 pyramidal neurons at $\sim$ 150 μm from the pial surface. A 150-200 μl solution of 12.5 μM 4-AP or an equal volume of vehicle (0.9% NaCl) was injected 1 mm antero-laterally to the imaged FoV at the level of the primary visual cortex (V1) at the infragranular layer ($\sim$ 600 μm deep from the pial surface). See Fig. 1. About 20 min after each injection, the post injection activity was recorded. Each recording lasts approximately 10 min. We have three different measurements for the same mouse: pre-injection (*control*), then post-vehicle injection, and post-4-AP injection. Here we report our preliminary analysis for the control and post 4-AP injection.

Deconvolution and thresholding The raw fluorescence signal of each neuron recorded through two photon microscopy is deconvolved using Vogelstein *et al.* Bayesian estimation algorithm [17]. The algorithm uses the df/f of

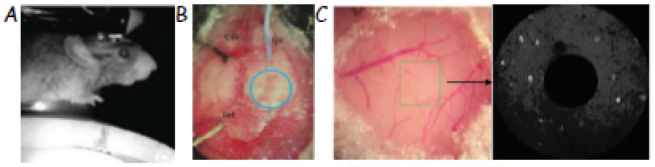

Fig. 1. A. The mouse is headposted rested awake and free to walk on a treadmill. B. Skull picture showing electrode implantation and site of planned window to overly visual cortex. C. (Left) Craniotomy window after implantation. Green frame illustrates the field of view (FOV). (Right) FOV (diameter $\sim 500\mu m$) showing spontaneous activity, scanned by the spiral scanning method.

the signal, which corresponds to the raw fluorescence signal minus the baseline of the signal over the baseline, where the baseline corresponds to the 10$^{\text{th}}$ percentile of the raw signal. The algorithm estimates the most probable spike train given the calcium concentration signal, assuming a linear dependence of the fluorescence and the calcium concentration, which decays exponentially to the calcium baseline upon excitation. It reports a continuous value representing the probability that a spike occurs at the corresponding frame. To transform it to eventogram, a threshold based on the *noise intervals* of the df/f is employed. Specifically, we form a Gaussian distribution with mean the 20$^{\text{th}}$ percentile of the neuron's df/f, using all the values that are less than this 20$^{\text{th}}$ percentile, "mirroring" their values at the right part of the synthetic distribution. The frames that are less than the mean plus the two standard deviations of this Gaussian distribution correspond to the noise intervals of that neuron. We then threshold the deconvolved signal based on the 99$^{\text{th}}$ percentile of the deconvolved signal values that lie in the noise intervals: a value higher than the threshold corresponds to spike (1), otherwise to no spike (0).

4. NETWORK ANALYSIS

Temporal correlation STTC quantifies the temporal correlation between spike trains. Specifically, for the estimation of the STTC between spike trains A and B, it computes the proportion of total recording time which lies within $\pm\Delta$t of any spike of the spike trains of A and B, T_A and T_B, respectively. Then, it computes the proportion of spikes from A, which lie within $\pm\Delta$t of any spike from B (P_A). P_B is calculated similarly. The spike time tiling coefficient can be defined by:

$$STTC = \frac{1}{2}\Big(\frac{P_a - T_b}{1 - P_a T_b} + \frac{P_b - T_a}{1 - P_b T_a}\Big) \qquad (1)$$

The normalization factor (1 - $P_a T_b$) ensures that STTC is in the range of [-1, 1]. The STTC is positive if spikes in train A are correlated with spikes from train B, and negative if there is less correlation than expected by chance.

For each pair of neurons (i,j), we estimate its (observed) STTC value ($STTC_{i,j}^{obs}$) as well as the null which corresponds to the chance level (null). For the estimation of the null, for each pair (i, j), we circularly shift j by a randomly selected number (in the range of $[1, T]$, where T is the length of the spike train), leading to spike train j'. Next, the STTC between i and j' is estimated. We repeat this process 500 times. This corresponds to the null distribution. The mean $\overline{STTC_{i,j}^{null}}$ and standard deviation $\sigma_{i,j}^{null}$ of the control, for each pair (i, j) are estimated. The neurons (i, j) have a statistical significant temporal correlation (i.e., are connected with an edge), if their STTC value $STTC_{i,j}^{obs}$ is above a certain z-value threshold, α (here 4).

We consider the *synchronous* firing of two neurons (i.e., two neurons exhibit a firing event *within the same frame*) as well as the *strictly directional* with lag approximately 0.2 sec (i.e., the firing of two neurons with lag of *exactly one* frame). Note that the strictly directional does *not* consider synchronous firing (co-firing within the same frame).

Affinity and Fast Belief Propagation BP combines weak signals to derive stronger ones, employing the principle of the "homophily" or influence of a node on its neighbors. Here we use the Fast Belief Propagation (FaBP) [9], an algorithm that yields twice speedup, equal or higher accuracy than BP, and is guaranteed to converge. It has been extended to weighted, directed networks using weighted non-symmetric adjacency matrices. The incorporation of STTC values in the form of edge weights can produce affinity values which capture more information about the role of the neurons in the network.

Connectivity characterization

Statistically significant temporal correlation in control and post 4-AP condition. The post 4-AP exhibits significant temporal correlations, stronger than the control, for both the synchronous case as well as the strictly directional with lag 1 (as shown in Figs 2, left and right, respectively). The differences of the post 4-AP vs. the control vs. null are prominent.

Dense functional connectivity in post 4-AP compared to the control. Compared to control, post 4-AP exhibits denser functional connectivity, as illustrated with the larger percentage of significant edges, clustering coefficient, and affinity metrics (99.78% vs. 42.20% (lag 0), 89.14% vs. 30.57% (lag 1)). The temporal correlation persists for strictly directional STTC with lag of one frame. Post 4-AP manifests strong functional connectivity, higher than that of the control, with high normalized degree of connectivity, and weighted directed clustering coefficients (Table 1 and Fig. 3).

Prominent differences of the post 4-AP compared to the other network topologies. The differences in the topology of the post 4-AP compared to the Erdös-Rényi (ER), Watts-Strogatz (WS), and null graphs are prominent. ER and WS graphs are constructed with the same number of nodes (252) and edges as the 4-AP graph with lag 1 frame; their edge

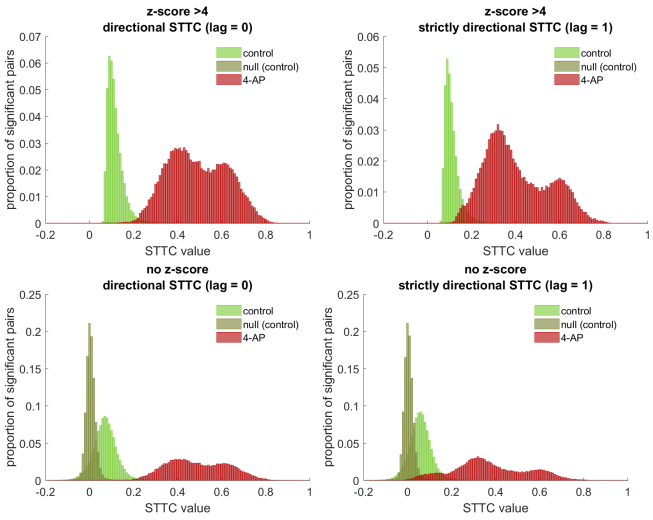

Fig. 2. STTC values for control and post 4-AP for STTC lag 0 (left) and 1 (right) normalized by the total number of possible edges for each case: (top) only statistically significant edges; null has a few edges and is not visible; (bottom) all edges included.

Table 1. (top) Median normalized DoC & WCC for control & post 4-AP; (bottom) Affinity for various graphs, equivalent to the post 4-AP (STTC, lag of 1 frame); KS test used.

Graph	DoC	WCC
4-AP	0.996 ± 0.084	0.932 ± 0.037
control	0.580 ± 0.305	0.391 ± 0.120

Graph	Median affinity ($\pm 2.sd$)	p-value
4-AP	0.2329 ± 0.0449	-
Null	0.1453 ± 0.0051	< 0.001
ER	0.1766 ± 0.0026	< 0.001
WS	0.1609 ± 0.0009	< 0.001
control	0.1563 ± 0.0102	< 0.001

weights were all set to the same value, equal to the mean STTC value of 4-AP graph. The corresponding statistically significant null graph was constructed as described before. In the control, a different number of nodes (350) was recorded. Table 1 (bottom) presents the median affinities of nodes of the corresponding graphs. The affinity vector of the 4-AP graph is statistically significantly different from the corresponding null, ER, WS graphs and control (p-values for significance of affinities estimated using the KS test).

The highest values of affinity of neurons in post 4-AP are identified in the lower half circle of the FoV, close to the area of the 4-AP injection (as shown in Figures 3(top)). Unlike the affinity, the weighted directed clustering coefficient here does not reveal any significant properties in the spatial distribution of neurons (Fig. 3(bottom)).

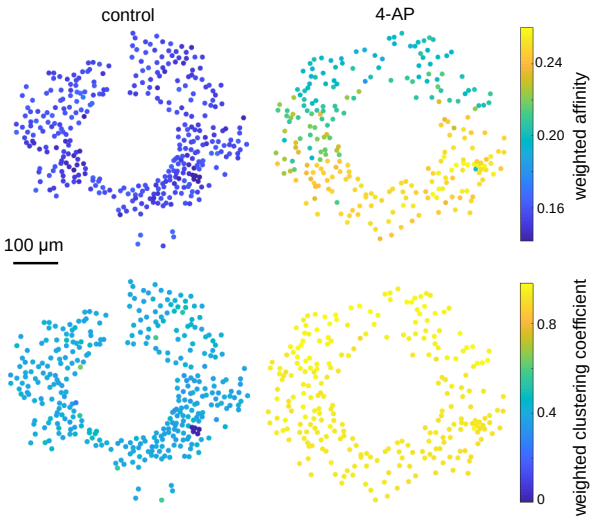

Fig. 3. Weighted directed affinity induces unsupervised clustering of neurons in 4-AP (lag of 1 frame) (top) in contrast to weighted directed clustering coefficient (bottom).

Comparing affinity to clustering coefficient Unlike in the case of 4-AP and control graphs without weights, where their affinity distributions at lag 1 had a small overlap (not shown here due to space constraints), the weighted affinity distributions of the corresponding graphs, i.e., integrated with the STTC weights, are well-separated. Moreover, the weighted affinity reveals an interesting localization property (Fig. 3(top)). Unlike clustering coefficient, which is a strictly local metric, the affinity captures the connectivity of a neuron along a larger area (e.g., within a range of 10-hop away neighbors) catching the more active neural network in the 4-AP condition. The lower part of the FoV is closer the area of the 4-AP injection.

5. CONCLUSIONS AND FUTURE WORK

This work demonstrated the high temporal correlation of neurons in the context of 4-AP and its denser functional network connectivity, compared to other network architectures and conditions. Moreover, it highlighted the power of the weighted affinity to identify neurons that seem to play an important role in the evolution of the ictogenesis. In contrast to clustering coefficient and normalized degree, the affinity can spot neurons that change most during epileptic seizure as evidenced by their proximity to the 4-AP injection site. Our future work will examine the time-evolving aspects of the 4-AP mechanism, and "label-tracking" over time. We plan to examine whether the EEG signal can reveal information about the states of other neurons (e.g., interneurons outside of the FoV) that may play important role in the propagation or in the control of seizures. The proposed metrics and methodology set a framework for the identification of the conditions that cause these seizures and their control: whether there exist special "gate" neurons that are reliably engaged, potentially orchestrating certain patterns.

6. REFERENCES

[1] V. Raymont, A.M. Salazar, R. Lipsky, D. Goldman, G. Tasick, and J. Grafman, "Correlates of posttraumatic epilepsy 35 years following combat brain injury," *Neurology*, vol. 75, no. 3, 2010.

[2] S.M. Sisodiya and H.C. Mefford, "Genetic contribution to common epilepsies," *Current opinion in neurology*, vol. 24, no. 2, 2011.

[3] M. Avoli et al., "Network and pharmacological mechanisms leading to epileptiform synchronization in the limbic system in vitro," *Progress in neurobiology*, vol. 68, no. 3, 2002.

[4] D. Hirtz, D. J. Thurman, K. Gwinn-Hardy, M. Mohamed, A. R. Chaudhuri, and R. Zalutsky, "How common are the "common" neurologic disorders?," *Neurology*, vol. 68, no. 5, 2007.

[5] A. Palagina, J.F. Meyer, and S. Smirnakis, "Inhibitory units: An organizing nidus for feature selective sub-networks in area V1," *Journal of Neuroscience*, 2019.

[6] J. K. Miller, I. Ayzenshtat, L. Carrillo-Reid, and R. Yuste, "Visual stimuli recruit intrinsically generated cortical ensembles," *Proceedings of the National Academy of Sciences*, vol. 111, no. 38, 2014.

[7] W. Ji, R. Gămănuţ, P. Bista, R. D. D'Souza, Q. Wang, and A. Burkhalter, "Modularity in the organization of mouse primary visual cortex," *Neuron*, vol. 87, no. 3, 2015.

[8] C. S. Cutts and S. J. Eglen, "Detecting pairwise correlations in spike trains: An objective comparison of methods and application to the study of retinal waves," *Journal of Neuroscience*, vol. 34, no. 43, 2014.

[9] D. Koutra, T.-Y. Ke, U. Kang, D. H. Chau, H.-K. K. Pao, and C. Faloutsos, "Unifying guilt-by-association approaches: Theorems and fast algorithms," in *Machine Learning and Knowledge Discovery in Databases*, 2011.

[10] J. Extercatte, G.n de Haan, and A. Gaitatzis, "Teaching video neuroimages: Frontal opercular seizures with jacksonian march," *Neurology*, vol. 84, no. 11, 2015.

[11] M. Wenzel, J. P. Hamm, D. S. Peterka, and R. Yuste, "Reliable and elastic propagation of cortical seizures in vivo," *Cell Reports*, vol. 19, no. 13, 2017.

[12] M. Wenzel, J. P. Hamm, D. S. Peterka, and R. Yuste, "Acute focal seizures start as local synchronizations of neuronal ensembles," *Journal of Neuroscience*, vol. 39, no. 43, 2019.

[13] L. F. Rossi, R. C. Wykes, D. M. Kullmann, and M. Carandini, "Focal cortical seizures start as standing waves and propagate respecting homotopic connectivity," *Nature Communications*, vol. 8, 2017.

[14] M. Kampourakis, A. Zacharakis, O. Mousouros, G. Palagina, J. Meyer, S. M. Smirnakis, I. Smyrnakis, and M. Papadopouli, "Functional network connectivity analysis in absence epilepsy using stargazer mice," in *2019 IEEE 19th International Conference on Bioinformatics and Bioengineering (BIBE)*, 2019.

[15] G. P. Clemente and R. Grassi, "Directed clustering in weighted networks: A new perspective," *Chaos Solitons & Fractals*, vol. 107, 2017.

[16] H. Dana, T.W. Chen, A. Hu, B. C. Shields, C. Guo, L. L. Looger, D. S. Kim, and K. Svoboda, "Thy1-gcamp6 transgenic mice for neuronal population imaging in vivo," *PLOS ONE*, vol. 9, 2014.

[17] J. T. Vogelstein, A. M. Packer, T. A. Machado, T. Sippy, B. Babadi, R. Yuste, and L. Paninski, "Fast nonnegative deconvolution for spike train inference from population calcium imaging," *Journal of Neurophysiology*, vol. 104, no. 6, 2010.